Chromosome Res (2016) 24:393–405
DOI 10.1007/s10577-016-9529-5

ORIGINAL ARTICLE

The distribution of α-kleisin during meiosis in the holocentromeric plant *Luzula elegans*

Wei Ma · Veit Schubert · Mihaela Maria Martis · Gerd Hause · Zhaojun Liu · Yi Shen · Udo Conrad · Wenqing Shi · Uwe Scholz · Stefan Taudien · Zhukuan Cheng · Andreas Houben

Received: 1 March 2016 / Revised: 3 May 2016 / Accepted: 5 May 2016 / Published online: 13 June 2016

Abstract Holocentric chromosomes occur in a number of independent eukaryotic lineages, and they form holokinetic kinetochores along the entire poleward chromatid surfaces. Due to this alternative chromosome structure, *Luzula elegans* sister chromatids segregate already in anaphase I followed by the segregation of the homologues in anaphase II. However, not yet known is the localization and dynamics of cohesin and the structure of the synaptonemal complex (SC) during meiosis. We show here that the α-kleisin subunit of cohesin localizes at the centromeres of both mitotic and meiotic metaphase chromosomes and that it, thus, may contribute to assemble the centromere in *L. elegans*. This localization and the formation of a tripartite SC structure indicate that the prophase I behaviour of *L. elegans* is similar as in monocentric species.

Keywords Holocentric chromosome · α-kleisin · Synaptonemal complex · *Luzula elegans* · CENH3

Abbreviations

dNTP	Deoxynucleoside triphosphates
PCR	Polymerase chain reaction
DNA	Deoxyribonucleic acid
SIM	Structured illumination microscopy

Responsible Editor: Jiming Jiang.

Electronic supplementary material The online version of this article (doi:10.1007/s10577-016-9529-5) contains supplementary material, which is available to authorized users.

W. Ma · V. Schubert · Z. Liu · U. Conrad · U. Scholz · A. Houben (✉)
Leibniz Institute of Plant Genetics and Crop Plant Research (IPK), Gatersleben, 06466 Stadt Seeland, Germany
e-mail: houben@ipk-gatersleben.de

M. M. Martis
Institute of Bioinformatics and Systems Biology/Munich Information Center for Protein Sequences, Helmholtz Center Munich, German Research Center for Environmental Health, 85764 Neuherberg, Germany

M. M. Martis
Division of Cell Biology, Department of Clinical and Experimental Medicine, Bioinformatics Infrastructure for Life Sciences, Linköping University, 558185 Linköping, Sweden

G. Hause
Biocenter, Microscopy Unit, Martin Luther University Halle-Wittenberg, Weinbergweg 22, 06120 Halle, Germany

Y. Shen · W. Shi · Z. Cheng
State Key Laboratory of Plant Genomics, Institute of Genetics and Developmental Biology, Chinese Academy of Sciences, 100101 Beijing, China

S. Taudien
Leibniz Institute on Aging-Fritz-Lipmann-Institut e.V. (FLI), Beutenbergstraße 11, 07745 Jena, Germany

SMC Structural maintenance of chromosome
SC Synaptonemal complex
RACE Rapid amplification of cDNA ends

Introduction

Accurate chromosome transmission is required for both the proliferative cell divisions in mitosis and the two sequential divisions in meiosis to reduce the genome copy number from two in diploid germline cells to one in haploid gametes. During these cell divisions, sister chromatids are held together at their arm and centromere regions by cohesin complexes. These complexes consist of different subunits: namely the structural maintenance of chromosome (SMC) 1 and SMC3 proteins, the α-kleisin SCC1 (also named RAD21 or REC8, see also Table 1) and the SCC3 protein (Nasmyth 2011). The subunits have been extensively studied in yeast, animals and human, but also homologs in plants have been characterized (reviewed in Schubert 2009). Biochemical and structural studies demonstrated that SCC1 simultaneously binds to SMC1 and SMC3 to form a tripartite ring proposed to mediate sister chromatid cohesion by encircling sister chromatids (reviewed in Nasmyth and Haering 2005). In almost all eukaryotes, SCC1 is present in the mitotic cohesin complex and replaced during meiosis by REC8 (Anderson et al. 2002; Cai et al. 2003; Golubovskaya et al. 2006; Pasierbek et al. 2001; Zhang et al. 2006). SCC1 is the main regulator of the cohesin complex at somatic anaphase.

During mitosis, most of the cohesins are degraded from the chromosome arms via phosphorylation of the SCC3 subunit by PLK1 before metaphase (Losada et al. 2002; Sumara et al. 2002). However, the centromeric cohesins are maintained until the anaphase onset when SCC1 is cleaved by the separase (Haering and Nasmyth 2003). In contrast to mitosis, during meiosis, two rounds of chromosome segregation follow a single replication step to generate haploid gametes. Thus, sister chromatid cohesins must be released in two steps during meiosis in monocentric species: (i) loss of chromatid arm cohesion between both homologues to release chiasmata and to enable reductional segregation during meiosis I (Kudo et al. 2006; Kudo et al. 2009) and (ii) the loss of sister centromere cohesion allows the sister chromatids to segregate during anaphase of meiosis II (Llano et al. 2008). However, the process of meiosis in organisms with holocentric chromosomes illustrates that

Table 1 Temporal appearance of meiotic α-kleisin subunits during the meiosis of different species

Species		Meiotic α-kleisin	Presence during meiosis	Reference
Common name	Scientific name			
Wood rush	*Luzula elegans* Lowe	Leα-kleisin	Leptotene to anaphase II	This study
Thale cress	*Arabidopsis thaliana replace by (no in ITALICS): (L.) Heynh.*	SYN1	Leptotene to metaphase I	Cai et al. (2003)
Tomato	*Solanum lycopersicum* (L.) H. Karst	REC8	Leptotene to diplotene	Qiao et al. (2011)
Rice	*Oryza sativa* L.	REC8, RAD21-4	Leptotene to diplotene	Shao et al. (2011), Zhang et al. (2006)
Nematode	*Caenorhabditis elegans* (Maupas, 1900)	REC8	Leptotene to the onset of anaphase I	de Carvalho et al. (2008)
Grasshopper	*Eyprepocnemis plorans* (Charpentier, 1825)	REC8	Zygotene to metaphase I	Valdeolmillos et al. (2007); Calvente et al. (2013)
Mouse	*Mus musculus* L.	RAD21	Leptotene to the end of anaphase II	Xu et al. (2004)
		REC8	Leptotene to metaphase II	Lee et al. (2003)
		RAD21L	Leptotene to the end of pachytene	Lee and Hirano (2011)
Rat	*Rattus norvegicus* (Berkenhout, 1769)	REC8	Leptotene to anaphase II	Eijpe et al. (2003)
Human	*Homo sapiens* L.	RAD21L	Leptotene to anaphase II	Herran et al. (2011)
		REC8	Leptotene to metaphase II	Garcia-Cruz et al. (2010)

our knowledge of meiotic chromosome arrangement and segregation based on observations of monocentric chromosomes may not apply to all organisms (Cabral et al. 2014; Heckmann et al. 2014a).

In principle, there are two options to release cohesins during holocentric meiosis: (i) such as in the nematode *Caenorhabditis elegans*, at a cruciform bivalent with a short (mid-bivalent) and a long arm. Spindle fibres attach to a restricted terminal chromosome region during metaphase I allowing the degradation of cohesion at the mid-bivalent and retention at the long arms during anaphase I enabling homologue separation. During meiosis II, cohesion at the sister chromatid interface gets lost allowing sister chromatid separation (Albertson and Thomson 1993; Nabeshima et al. 2005; Kaitna et al. 2002); (ii) in other holocentric species such as the wood rush *Luzula elegans*, an inverted sequence of meiotic sister chromatid segregation occurs (Fig. 3). In contrast to monopolar sister centromere orientation in monocentric species, the unfused holokinetic sister centromeres behave as two distinct functional units during meiosis I, resulting in sister chromatid separation. Homologous non-sister chromatids remain terminally linked after metaphase I until metaphase II. Then, they separate at anaphase II (Heckmann et al. 2014a). Therefore, it is expected that the degradation of cohesins during holocentric meiosis may deviate from that of monocentric species. However, the dynamics and function of cohesin during this process are not yet known.

Besides releasing sister chromatid cohesion, cohesin complexes also participate in the assembly of the synaptonemal complex (SC) (Klein et al. 1999; Hartsuiker et al. 2001). The SC consists of a proteinaceous structure, the axial element (AE) mediating the association of each pair of homologous sister chromatids. After pairing, the AEs become associated by transverse filaments to the central element (CE) to establish the tripartite SC. The SC provides the structural framework for synapsis, double-strand break repair and exchange between homologues (Henderson and Keeney 2005). However, unknown is whether the SC complex structure is conserved in holocentric species such as *L. elegans*.

In this work, we aimed to delve deeper into the organization of holocentric chromosomes. We found that α-kleisin at both mitotic and meiotic metaphase chromosomes colocalizes with the centromere and may contribute to the assembly of the centromere. This localization of α-kleisin and the formation of a tripartite SC structure indicate that the prophase I behaviour of *L. elegans* is similar as in monocentric species.

Materials and methods

Plant material and plant cultivation

L. elegans Lowe (2n = 6) (Vouchers at the Herbarium Gatersleben: GAT 7852–7856) plants were cultivated for 4 weeks under short-day conditions (8-h light/16-h dark, 20 °C/18 °C) and then vernalized (10-h light/14-h dark, 4 °C) for at least 4 weeks. The plants were finally grown under long-day conditions (16-h light, 22 °C day/16 °C night), and all experimental materials from different tissues were collected during this period.

RNA extraction, RT-PCR and qRT-PCR

Total RNA was extracted from leaves, stems and flower buds by the TRIzol method (Life Technologies). The RNA samples were treated with RNA-free DNase I (Ambion TURBO DNase; Invitrogen) before complementary DNA (cDNA) synthesis. The absence of genomic DNA was confirmed by PCR with the *LeGAPDH*-specific primers G1F and G1R (Supplemental Table 1). All cDNAs (20 μl) were generated from 1 μg DNase I-treated RNA, using the Reverse Aid H Minus First Strand cDNA Synthesis Kit (Fermentas). cDNAs used for 5′- and 3′- RACE PCR were synthesized from messenger RNA (mRNA) of flower buds according to the SMART RACE cDNA Amplification Kit (Clontech, Palo Alto, CA) manual protocol.

Twenty-five-microliter PCR reaction mixtures contained the following: 1 μl cDNA, 10 μM of each forward and reverse primers (Supplemental Table 1), 5 mM of each deoxynucleotide triphosphates, 2.5 μl 10× PCR reaction buffer and 1 unit of *Taq* polymerase (Qiagen). The cycling protocol was as follows: 94 °C for 3 min, 35 cycles (at 94 °C for 40 s, 58 °C for 40 s, 1 min/kb elongation at 72 °C) and 72 °C final elongation for 10 min. Twenty-five PCR cycles were run with *LeGAPDH*-specific primers (G1F and G1R, Supplemental Table 1) to quantify the abundance of transcripts. 5′- and 3′-RACE PCRs were performed according to the SMART RACE cDNA Amplification Kit (Clontech, Palo Alto, CA) manual protocol.

Quantitative reverse transcription PCR (qRT-PCR) was performed using the SYBR Green Master mix (Applied Biosystems) on the 7900HT Fast Real-Time PCR System (Applied Biosystems). Ten microliters of PCR mixture contained 0.2 μl of cDNA template, 5 μl of 2× Power SYBR Green PCR Master Mix (Applied

Biosystems) and 0.33 mM of the forward and reverse primers (Supplemental Table 1) for each gene. The amplification conditions were one cycle at 95 °C for 10 min, 40 cycles of two consecutive steps at 95 °C for 15 s and at 60 °C for 60 s. *LeGAPDH*-specific primers G2F and G2R (Supplemental Table 1) were used as endogenous control.

RNAseq and de novo assembly

Total RNA was isolated from *L. elegans* pollen mother cells using the Spectrum™ Plant Total RNA Kit (Sigma) according to the manufacturer's instruction followed by cDNA Illumina paired-end library preparation (Vertis Biotechnologie AG, Freising, Germany). The library was sequenced (one lane, 2× 100 bp) on an Illumina HiSeq 2000, resulting in 81.2 million read pairs which were assembled. The pollen mother cell transcriptome of *L. elegans* can be used for BLAST search under: http://webblast.ipk-gatersleben.de/luzula/.

Sequence analysis

DNA fragments were sequenced by the service facility of the IPK (Gatersleben, Germany). Sequences were analyzed by Sequencher 5.2.4 (Gene Codes Corporation Inc), assembled using Seqman pro 12.0.0 (DNASTAR, Inc) and processed by EditSeq and MegAlign Lasergene 8 (DNASTAR, Inc). Reference IDs for the phylogenetic analysis of the α-kleisin sequences used in this study are available in Supplemental Table 2, and CENH3 sequences used for comparison are described in Marques et al. (2015). Phylogenetic trees were constructed by the software Geneious (version 7.0.6; http://www.geneious.com).

Total protein extraction and Western blot analysis

For isolation of total *L. elegans* proteins, 200 mg of grinded flower buds were suspended in 250 µl extraction buffer (112 mM Na_2CO_3, 112 mM DTT, 4 % SDS, 24 % sucrose, 4 mM EDTA and 1 mg 3,3,5,5-tetrabromophenolsulfonephthalein) and kept at 65 °C for 20 min. After centrifugation at 14,000 rpm for 5 min at 4 °C, the supernatant contained the total soluble proteins.

The proteins were separated by 10 % (*w*/*v*) polyacrylamide gels according to Schägger and Von Jagow (1987); then, the gels were blotted on Immobilon PVDF membranes (Millipore). These membranes were incubated first with primary antibodies (1:1000 rabbit anti-LeCENH3, 1:5000 rabbit anti-histone H3 (Sino Biological Inc., 100005-MM01-50) and 1:5000 mouse anti-α tubulin (clone DM 1A, Sigma) and then with the corresponding secondary antibodies [1:5000 anti-rabbit IgG IRDye 800CW (LI-COR, 925-32213) or 1:5000 anti-mouse IgG IRDye 680RD (LI-COR, 926-32222)]. The immunoblots were imaged using a LI-COR Odyssey Imager. Histone H3 and α-tubulin signals were used as controls.

Antibody production

To generate antibodies against Leα-kleisin, a 1017-bp fragment of Leα-kleisin (primers R1F and R1R, Supplemental Table 1) was amplified from flower bud cDNA. The fragments were cloned into the vector pSC-A-amp/kan using the StrataClone PCR cloning kit (Stratagene), sequenced and then sub-cloned into the expression vector pET-23a-d(+) (Novagen). The resulting pET-23a-Leα-kleisin construct was transformed into *Escherichia coli* BL21 (DE3), and the expression of proteins was induced by 1 mM isopropylthio-beta-D-galactoside (IPTG). The Leα-kleisin recombinant proteins were purified under native condition on Ni-NTA agaroses (Qiagen) and then confirmed by Western blot using mouse monoclonal anti-His-tag (1:1000, Millipore, 05-949) and 1:5000 anti-mouse IgG IRDye 680RD (LI-COR, 926-32222) antibodies. A polyclonal rabbit anti-Leα-kleisin antibody was produced by Pineda (Antikörper-Service, Berlin, Germany). The specificity of anti-Leα-kleisin antibody (1:1000) was checked on a Western blot with recombinant proteins. The method for Western blot is described above.

For the generation of LeCENH3-specific antibodies, an epitope corresponding to the N-terminal end of LeCENH3 (3-RTKHFSNRKSIPPKKQTPAK-23) was identified. Peptide synthesis, immunization of rabbits and peptide affinity purification of antisera were performed by LifeTein LLC (South Plainfield, NJ, USA).

Indirect immunostaining and light microscopy

Indirect immunostaining of *L. elegans* was performed as described by Heckmann et al. (2014a), of *Hordeum vulgare* and *Vicia faba* as described by Schubert et al. (1993). The following primary antibodies were used: rabbit anti-Leα-kleisin (1:100), mouse anti-OsSgo1 (1:200) (Wang et al. 2011), guinea pig anti-ZmZYP1 (1:100) (Golubovskaya et al. 2011), rabbit anti-grass

CENH3 (1:300) (Sanei et al. 2011) and rabbit anti-LeCENH3 (1:100). Texas red-conjugated anti-rabbit antibodies (1:400) (Molecular Probes), fluorescein isothiocyanate-conjugated anti-mouse antibodies (1:300) (Molecular Probes) and Alexa 488-conjugated anti-guinea pig (1:300) (Dianova) antibodies were used as secondary antibodies. Anti-LeCENH3 and anti-grass CENH3 antibodies were directly labelled by the Fluorescein Labeling Kit-NH2 (Dojindo, LK01-10).

Images were collected in gray scale using an Olympus BX61 microscope (Olympus; http://www.olympus.com) and an ORCA-ER CCD camera (Hamamatsu; http://www.hamamatsu.com), then pseudocoloured and merged with Adobe Photoshop CS5 (Adobe). To achieve a lateral optical resolution of ~120 nm (super-resolution, obtained with a 488-nm laser), we applied structured illumination microscopy (SIM) using a 63x/1.4 Oil Plan-Apochromat objective of an Elyra PS.1 microscope system and the software ZEN (Carl Zeiss GmbH). Images were captured separately for each fluorochrome using the 561-, 488- and 405-nm laser lines for excitation and appropriate emission filters (Weisshart et al. 2016).

Electron microscopy

For transmission electron microscopy, cut-opened anthers undergoing prophase I were fixed for 4 h in 3 % glutaraldehyde (Sigma, Taufkirchen, Germany) in 0.1 M sodium cacodylate buffer pH 7.2 (SCB), washed, postfixed for 1 h with 1 % osmium tetroxide (Carl Roth, Karlsruhe, Germany) in SCB, dehydrated in a graded series of ethanol and embedded in epoxy resin according to Spurr (1969). Ultrathin sections (70 nm) were transferred to formvar coated grids and poststained with uranyl acetate and lead citrate. Subsequently, the grids were observed with an EM 900 (Carl Zeiss Microscopy, Oberkochen, Germany) transmission electron microscope (acceleration voltage 80 kV). Electron micrographs were taken with a slow scan camera (Variospeed SSCCD camera SM-1k-120, TRS, Moorenweis, Germany) using the iTEM software from Olympus SIS (Münster, Germany).

Accession numbers

Sequence data from this article can be found in the GenBank/EMBL data libraries under accession numbers PRJEB12761, *LeCENH3* gDNA (KT932953), *LeCENH3.1* mRNA (KT932953), *LeCENH3.2* mRNA (KT932954) *Leα-kleisin-1* mRNA (KT932948), *Leα-kleisin-2* mRNA (KT932949), *Leα-kleisin-3* mRNA (KT932950) and *Leα-kleisin-4* mRNA (KT932951).

Results

Identification of the centromere-specific histone H3 variant CENH3 in *L. elegans*

First, a *L. elegans*-specific centromere antibody recognizing the centromere-specific histone H3 (CENH3) was established. Both CENH3 variants of *Luzula nivea* (GenBank BAE026 and ADM18965) (Nagaki et al. 2005; Moraes et al. 2011) were used as query to identify the corresponding gene in the established RNAseq database of *L. elegans* pollen mother cells (http://webblast.ipk-gatersleben.de/luzula/). To determine the start and end of the *LeCENH3* transcript, 3′-RACE and 5′-RACE experiments were performed based on a 55-amino acid fragment showing high similarity to the C-terminal part of *L. nivea* CENH3 (Supplemental Fig. 1a, b). Cloning of the 5′-RACE products revealed two gene splicing variants (called *LeCENH3.1* and *LeCENH3.2*). *LeCENH3.2* differs from *LeCENH3.1* by having 21- and 3-bp-long deletions near the 5′-terminal part (Supplemental Fig. 1a). The full sequences of *LeCENH3.1* and *LeCENH3.2* were confirmed after PCR and RT-PCR using the primer pair C4F/C4R (Supplemental Fig. 1a). Phylogenetic analysis grouped both LeCENH3 variants together with the CENH3s of other *Juncaceae* species in a sister branch of monocots (Supplemental Fig. 1c).

Both *LeCENH3* splicing variants show a higher expression in flower buds than in stems and leaves as revealed by quantitative RT-PCR using the primer combinations (C2F/C2R and C3F/C2R). *LeCENH3.1* exhibited a higher expression than *LeCENH3.2* in flower buds and stems. In leaves, the activity of both was almost identical (Fig. 1a). But, a diverging expression was found in anthers by sequencing the cloned 5′-RACE products. Of the products, 74 % and only 26 % ($n = 38$) originated from *LeCENH3.1* and *LeCENH3.2*, respectively.

Next, a rabbit anti-LeCENH3 antibody was raised against a synthetic peptide containing the N-terminal 20 amino acid residues of both CENH3s (Supplemental Fig. 1b). To determine the antibody specificity, a Western blot assay was performed using the affinity-purified antibodies as probe on total protein extracts from flower

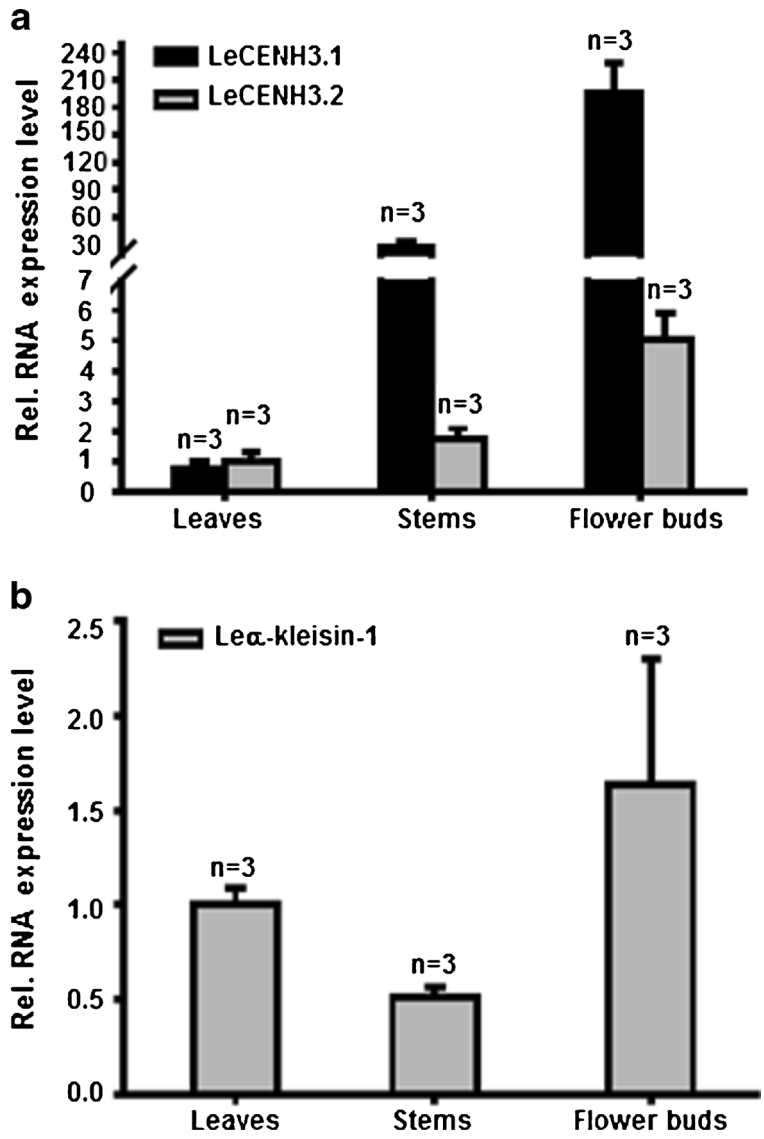

Fig. 1 Quantitative analysis of *LeCENH3* and *Leα-kleisin-1* transcripts in different tissues. **a** The relative transcription level of *LeCENH3.1* and *LeCENH3.2* was measured by qRT-PCR. **b** The total transcription level of *Leα-kleisin-1* in leaves, stems and flower buds was measured by qRT-PCR. The number of biological replicates is indicated above the standard deviation bars

buds of *L. elegans*. The major band fitted to the expected size of 20 kD (Supplemental Fig. 1d).

Identification of the *L. elegans* α-kleisins

To identify the α-kleisin subunits of *L. elegans* cohesin, we searched by BLASTP in the *L. elegans* RNAseq database using the Rad21/Rec8-like sequences of rice (Zhang et al. 2004) as query and identified in silico four α-kleisin-like genes. The phylogenetic analysis of the different monodicot and eudicot Rad21/Rec8 proteins indicated that each of the four *L. elegans* α-kleisin-like proteins was categorized into different subfamilies (Supplemental Fig. 2a), namely Leα-kleisin-1, Leα-kleisin-2, Leα-kleisin-3 and Leα-kleisin-4. The alignment of these four incomplete proteins revealed an overall similarity of only 8.3 to 36.8 % (Supplemental Table 3). However, the conserved N-terminal regions showed a higher similarity with 25.8 to 46.8 % (Supplemental Fig. 2b).

We chose Leα-kleisin-1 for further analysis, because this protein possibly represents an ortholog of the *Arabidopsis thaliana* α-kleisin SYN4 required for cohesion along chromosome arms and at centromeres (Schubert et al. 2009). In order to determine the transcription dynamics

of *Leα-kleisin-1*, cDNAs derived from stems, leaves and flower buds were used to perform qRT-PCR (primers R2F/R2R) (Supplemental Fig. 2c). As shown in Fig. 1b, the highest level of expression was found in flower buds. This agrees to data obtained for *Rad21-1* of rice (Zhang et al. 2004).

To test the chromosomal distribution of Leα-kleisin-1, rabbit polyclonal antibodies were raised against a partial recombinant Leα-kleisin-1 protein. We cannot exclude that these antibodies recognize also other members of the α-kleisin family since the N-terminal part is conserved. Therefore, we named the antibodies 'anti-Leα-kleisin'. The molecular

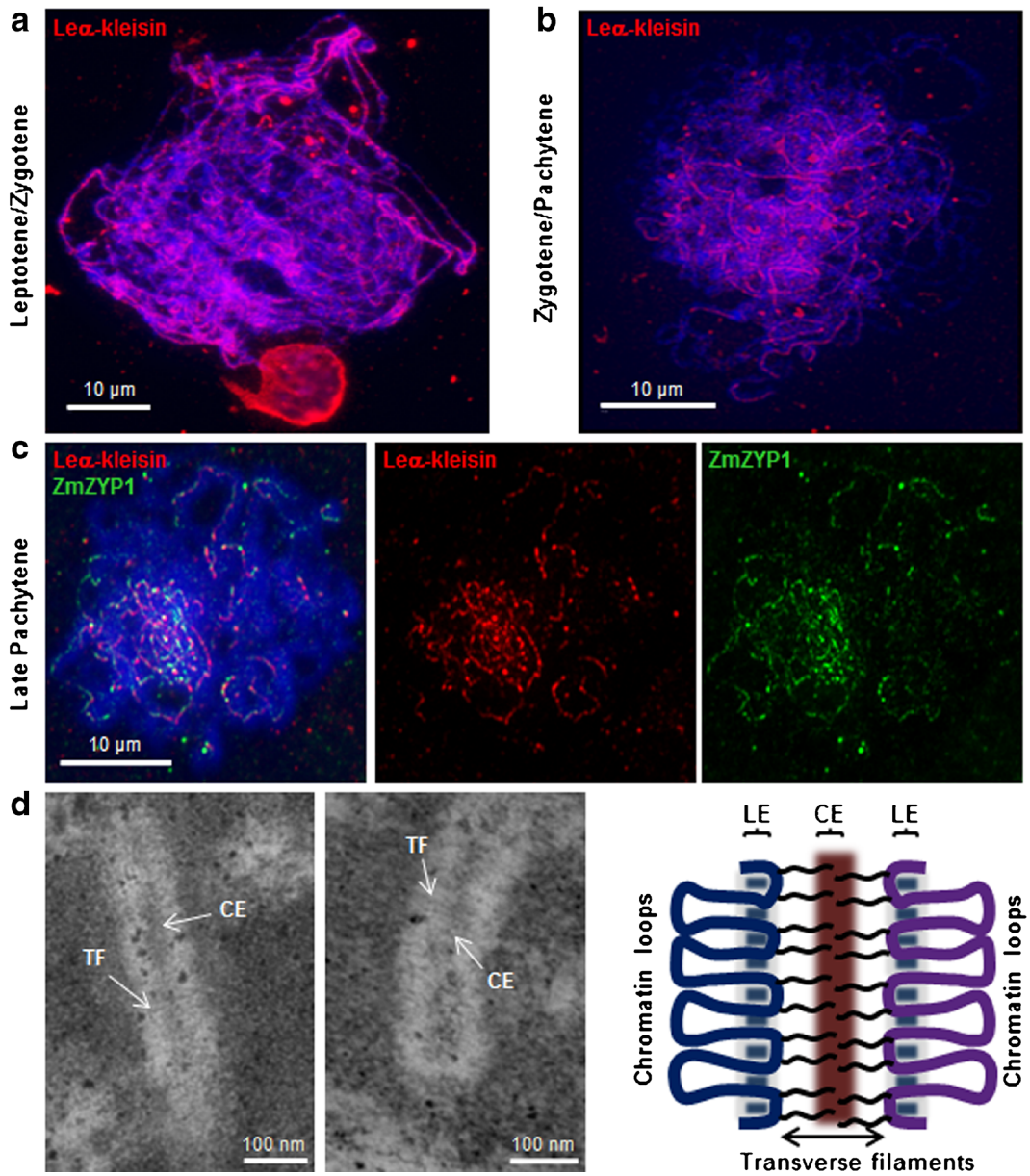

Fig. 2 Prophase I is conventional in the holocentric species *L. elegans*. **a**–**c** The distribution of Leα-kleisin from leptotene to late pachytene. **c** Colocalization of Leα-kleisin and ZmZYP1 at pachytene. **d** Electron micrographs of two *L. elegans* synaptonemal complexes (*left*), with the scheme of a synapsed homologous chromosome pair (*right*), in which the central element (CE) and putative transverse filaments (TF) indicated

weight of the recombinant protein used for antibody production was ~55 kDa (Supplemental Fig. 2d), although the expected size is 38 kDa. Such a difference was also observed for antibodies established against α-kleisin orthologs of mouse (Lee and Hirano 2011), *C. elegans* (Birkenbihl and Subramani 1995) and budding yeast (Michaelis et al. 1997), likely due to the high polarity of the proteins. Nevertheless, the cross-reaction of anti-Leα-kleisin with antigens produced by *E. coli* confirmed its specificity (Supplemental Fig. 2e).

Prophase I is conventional in *L. elegans*

Anti-Leα-kleisin staining was performed on pollen mother cell chromosomes to decipher the distribution of α-kleisin in prophase I. Leα-kleisin signals lined up into continuous structures during leptotene/zygotene (Fig. 2a, b). Double immunostaining with ZmZYP1 and Leα-kleisin antibodies showed that Leα-kleisin mainly localized in the ZmZYP1-positive regions during zygotene/pachytene (Fig. 2c). In addition, it was found that Leα-kleisin colocalizes to LeCENH3 during this stage (Supplemental Fig. 3). Thus, the distribution of meiotic cohesin during prophase I seems to be as similar as reported for monocentric species (Qiao et al. 2011).

To decipher whether a tripartite structure of the SC can be observed in *L. elegans*, we examined pachytene cells by transmission electron microscopy. We identified a 111.6 ± 10.6 nm-wide ($n = 20$) SC comprising a dense central region traversed by thin filaments (Fig. 2d). Surrounded by chromatin, the SC lies "zipper-like" along the central axis of the bivalent (Fig. 2d). These findings indicate that the SC structure of holocentric species is similar to those of monocentrics.

Leα-kleisin colocalizes with the centromeres of condensed chromosomes

In *L. elegans*, sister chromatid cohesion becomes already resolved during metaphase I (Heckmann et al. 2014a). However, the dynamics and function of cohesin during meiosis are not yet known. Therefore, we investigated the distribution of Leα-kleisin by immunostaining and found that it is present only in the centromere regions of metaphase I and II chromosomes (Fig. 3b, c). Super-resolution microscopy of metaphase I and II chromosomes labelled with anti-Leα-kleisin and anti-LeCENH3 revealed a close proximity of both proteins. In addition, antibodies against rice Shugoshin-specific (OsSGO1) were used as markers for cohesion. OsSGO1 stabilizes the SC and protects centromeric cohesion during the meiosis of rice (Wang et al., 2011). However, in *L. elegans*, we found that SGO1 was exclusively located in the holocentromeres of metaphase II chromosomes (Supplemental Fig. 4).

Leα-kleisin was also located at the holocentromeres of somatic *L. elegans* metaphase chromosomes, but not in regions where sister chromatids attach (Fig. 4a). In monocentric metaphase chromosomes of *H. vulgare* (Fig. 4b), Leα-kleisin signals appeared not only at the CENH3-positive regions, but also in between the sister chromatids. In *V. faba* (Supplemental Fig. 5), two separate Leα-kleisin signals were only present in the primary constrictions.

In summary, the results suggest that the α-kleisins of *L. elegans* may not only realize sister chromatid cohesion; instead, they colocalize with the position of the centromere. Additional experiments are required to prove the involvement of α-kleisins in the assembly of the centromeres in this species.

Discussion

The CENH3 of *L. elegans*

Whereas, in the closely related species *L. nivea*, two *CENH3* isoforms are present (Nagaki et al. 2005; Moraes et al. 2011), only one was found in *L. elegans*. But, interestingly, two different *LeCENH3* splicing variants with a tissue-specific expression pattern are evident. Similarly, two pearl millet (Ishii et al. 2015) and human CENH3 (also called CENP-A) (Gerhard et al. 2004) splicing variants were proven. However, no different functions of these variants have been determined until now. By immunostaining, we confirm previous findings (Heckmann et al. 2011; Heckmann et al. 2014a) that somatic *L. elegans* chromosomes contain a CENH3-positive longitudinal centromere along each sister chromatid and that holocentricity is maintained, and no fusion of sister centromeres occurs throughout meiosis.

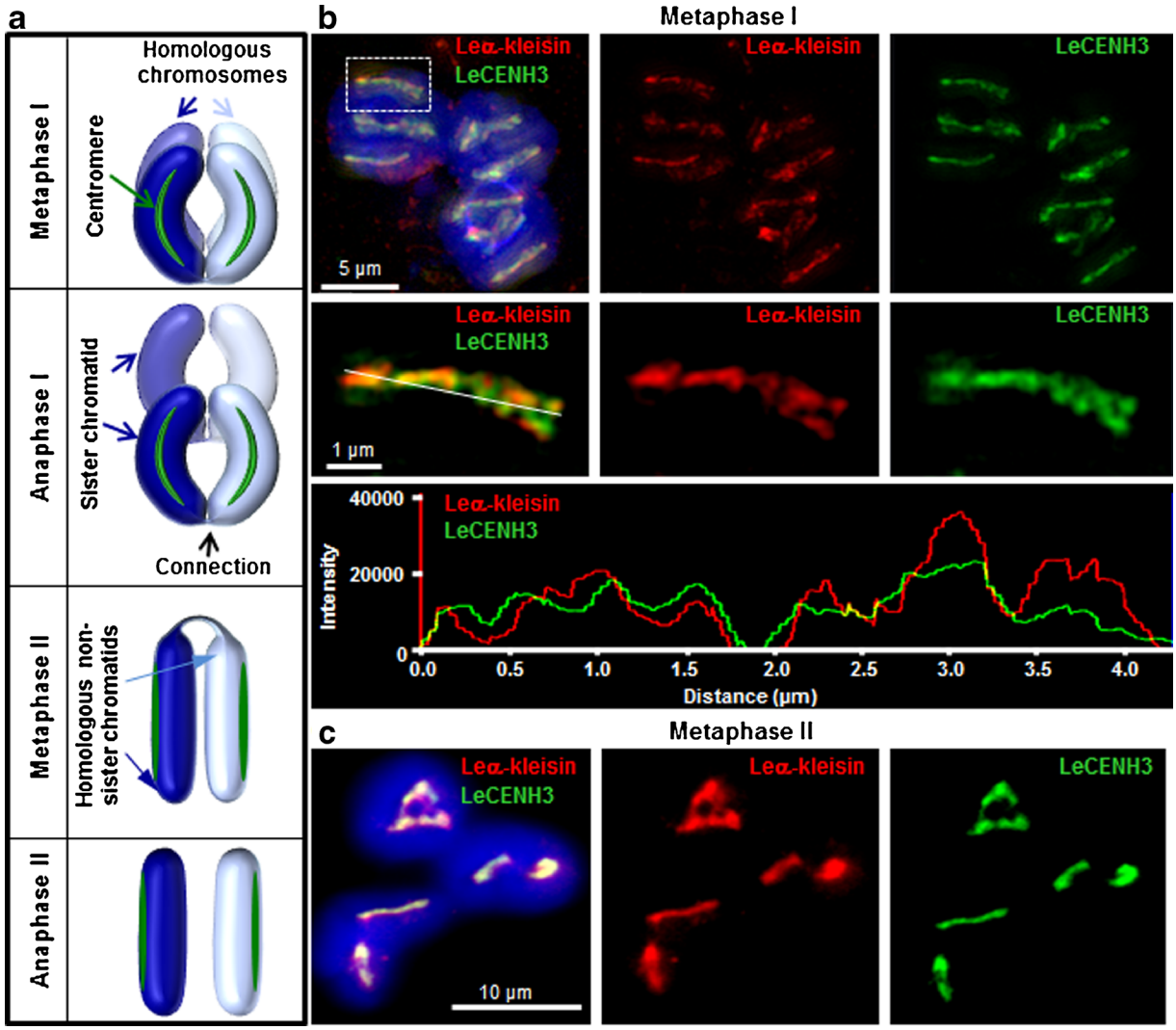

Fig. 3 Distribution of Leα-kleisin and LeCENH3 at meiotic metaphase I and II chromosomes of *L. elegans*. **a** Schematic model of meiosis in the holocentric species *L. elegans*. The U-shaped bivalents are aligned at metaphase I, and the sister chromatids separate already during anaphase I. Homologous non-sister chromatids are connected at their termini until metaphase II. Then, they separate at anaphase II. **b** The colocalization of Leα-kleisin and LeCENH3 at metaphase I centromeres was identified by SIM after immunostaining (*top*). The *middle panel* shows a region of interest (*rectangle*) further magnified. The quantification of centromeric fluorescence intensities of Leα-kleisin and anti-LeCENH3 from line scans of a single optical section is indicated (*below*). **c** The colocalization of Leα-kleisin and LeCENH3 at the centromeres of a single metaphase II daughter cell

α-Kleisins colocalize with the centromere

In *L. elegans*, four α-kleisins (Leα-kleisin-1-4) were identified. Based on our phylogenetic analysis, they correspond to those of other plants like *A. thaliana* (AtSYN1-4) and *Oryza sativa* (OsRad21-1-4) as follows: Leα-kleisin-4/AtSYN1/OsRad21-4, Leα-kleisin-2/AtSYN2/OsRad21-2, Leα-kleisin-3/AtSYN3/OsRad21-3 and Leα-kleisin-1/AtSYN4/ OsRad21-1 (da Costa-Nunes et al. 2006; Dong et al. 2001; Zhang et al. 2004; Zhang et al. 2006; Tao et al. 2007; Gong et al. 2011), in which the Leα-kleisin-4/AtSYN1/OsRad21-4 α-kleisins act during meiosis.

In the holocentric nematode *C. elegans*, also four different α-kleisin proteins (COH-1, COH-2, COH-3 and the meiotic REC-8 α-kleisin) were identified (Mito et al. 2003). In contrast, yeast contains only two α-kleisins, the mitotic SCC1 and the meiosis-specific variant REC8 (Lee and Orr-Weaver 2001). In mammals, three α-kleisins, RAD21, REC8 and RAD21L, were reported (Ishiguro

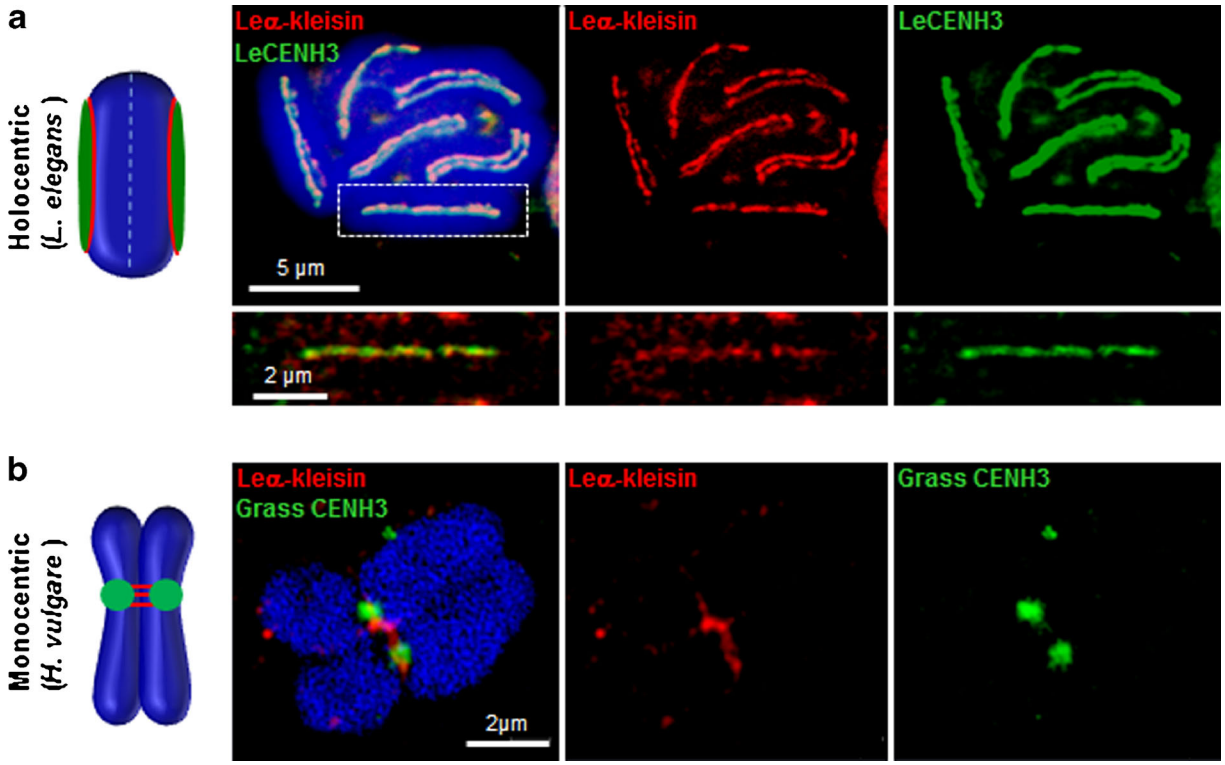

Fig. 4 Distribution of Leα-kleisin and CENH3 at mitotic metaphase chromosomes of *L. elegans* (**a**) and *H. vulgare* (**b**). **a** The holocentric species *L. elegans* shows clearly a colocalization of Leα-kleisin and LeCENH3 after immunostaining with specific antibodies. The *below panels* show regions of interest (*rectangle*) further magnified after applying SIM. **b** A monocentric *H. vulgare* chromosome acquired by SIM shows the Leα-kleisin in between of both sister centromeres, which are marked by two distinct CENH3 signals. The schemata on the *left side* compare the centromere arrangement and localization of Leα-kleisin (*red*) and CENH3 (*green*) in *L. elegans* (**a**) and *H. vulgare* (**b**) chromosomes

et al. 2011; Nasmyth 2011). In *A. thaliana*, it was proven that the four α-kleisin proteins have different functions (reviewed in Schubert 2009). SYN1 mediates cohesion during meiosis (Bhatt et al. 1999; Cai et al. 2003) and in differentiated interphase nuclei (Schubert et al., 2009). SYN2 and SYN3, mainly expressed in meristematic tissues, seem to be mitotic α-kleisins (Dong et al. 2001). SYN3 is enriched in the nucleolus; therefore, its additional involvement in controlling rDNA structure and transcription and its involvement in rRNA processing have been suggested (Jiang et al. 2007). SYN3 and SYN4 also support sister chromatid cohesion in differentiated interphase nuclei (Schubert et al., 2009). In agreement with the findings in vertebrates (Waizenegger et al. 2000), here, we show that α-kleisins may mediate sister chromatid cohesion during mitosis in monocentric species as *H. vulgare*, since we observed that α-kleisin remained between the sister centromeres during metaphase. Previous studies (Suzuki et al. 2013) did not prove plant cohesins at somatic metaphase chromosomes, which may be caused by an insufficient sensitivity of the antibodies used, by the image acquisition applied or by the preparation methods employed.

We found that α-kleisin is present along each metaphase sister centromere in *L. elegans*. This is in agreement with the distribution of RAD21L in mice, where two separate signals appear at the primary constrictions during metaphase II (Herran et al. 2011). Therefore, we support the assumption of Herran et al. (2011) that the enrichment of α-kleisin at centromeres may contribute to the assembly of the inner centromere and that it may play a role in promoting the bi-orientation of kinetochores (Sakuno et al. 2009).

In *L. elegans*, between metaphases I and II, the chromosomal termini of the homologous non-sister chromatids are connected to each other by chromatin threads. This allows to proceed an inverted sequence of meiotic sister chromatid segregation, and it was assumed that cohesins are involved in this end-to-end association (Heckmann et al.

2014b). However, here, we show that α-kleisin-containing cohesin complexes obviously are not involved in maintaining these connections.

The meiotic prophase I is conventional in *L. elegans*

Here, we report that Leα-kleisins localize exclusively from leptotene to pachytene along the axial and lateral elements of the SC. This is consistent with the finding that REC8 and HIM3, components of the chromosome axes, are required for meiotic synapsis in holocentric nematodes during leptotene, zygotene and pachytene (Zetka et al. 1999). This suggests that REC8 is a component of axial/lateral elements (Pasierbek et al. 2001). In plants, a specific and intermittent localization of SMC3 in the axial/lateral elements has been observed in tomato by electron microscopy in microsporocytes during zygotene, similar to that observed by light microscopy after the immunolabelling of SMC1, SMC3, SCC3 and REC8, although not all subunits presented the same pattern of accumulation and appearance during prophase I (Qiao et al. 2011). Also, a correlation between the progression of axial or lateral element formation and synapsis and the localization of several cohesin subunits was observed in many different monocentric species (Calvente and Barbero 2012). Although, till now, no functional analysis regarding the participation of cohesin during SC formation and synapsis is available in *L. elegans*, the sequential α-kleisin loading indicates a role in the correct progression of synapsis.

We report here that the synaptonemal complex of *L. elegans* is similar in structure and function as in other species (Goldstein 1987; Sym et al. 1993; Page and Hawley 2003). The width of the central region of the SC is ~111 nm in *L. elegans*. This is consistent with the data reported for other plants (Westergaard and von Wettstein 1972) and of *C. elegans* (Smolikov et al. 2008). Because the Leα-kleisins show a similar dynamic pattern during prophase I as monocentric species (Table 1), we conclude that their function during the SC formation is also conserved in holocentrics.

Acknowledgments We are grateful to all members of the Chromosome Structure & Function laboratory (IPK Gatersleben), Ingo Schubert (IPK) and E-Eva Tomaštíková (Centre of the Region Haná for Biotechnological and Agricultural, Research, Institute of Experimental Botany, Olomouc, Czech Republic) for fruitful discussions; to Karla Meier, Katrin Kumke, Oda Weiß, Isolde Tillack and Gresch Ulrike (IPK) for excellent technical assistance; to Anne Fiebig for sequence submission; and to Karin Lipfert (IPK) for help with artwork. This work was supported by the China CSC scholarship, the Deutsche Forschungsgemeinschaft (SPP 1384, HO 1779/17-1) and the IPK Gatersleben.

References

Albertson DG, Thomson JN (1993) Segregation of holocentric chromosomes at meiosis in the nematode, *Caenorhabditis elegans*. Chromosom Res 1:15–26

Anderson DE, Losada A, Erickson HP et al (2002) Condensin and cohesin display different arm conformations with characteristic hinge angles. J Cell Biol 156:419–424

Bhatt AM, Lister C, Page T et al (1999) The DIF1 gene of *Arabidopsis* is required for meiotic chromosome segregation and belongs to the REC8/RAD21 cohesin gene family. Plant J 19:463–472

Birkenbihl RP, Subramani S (1995) The rad21 gene product of *Schizosaccharomyces pombe* is a nuclear, cell cycle-regulated phosphoprotein. J Biol Chem 270:7703–7711

Cabral G, Marques A, Schubert V et al (2014) Chiasmatic and achiasmatic inverted meiosis of plants with holocentric chromosomes. Nat Commun 5:5070

Cai X, Dong F, Edelmann RE, Makaroff CA (2003) The *Arabidopsis* SYN1 cohesin protein is required for sister chromatid arm cohesion and homologous chromosome pairing. J Cell Sci 116:2999–3007

Calvente A, Barbero JL (2012) Cohesins and cohesin-regulators in meiosis. INTECH Open Access Publisher

Calvente A, Viera A, Parra MT et al (2013) Dynamics of cohesin subunits in grasshopper meiotic divisions. Chromosoma 122: 77–91

da Costa-Nunes JA, Bhatt AM, O'Shea S et al (2006) Characterization of the three *Arabidopsis thaliana* RAD21 cohesins reveals differential responses to ionizing radiation. J Exp Bot 57:971–983

de Carvalho CE, Zaaijer S, Smolikov S et al (2008) LAB-1 antagonizes the Aurora B kinase in *C. elegans*. Genes Dev 22:2869–2885

Dong F, Cai X, Makaroff C (2001) Cloning and characterization of two *Arabidopsis* genes that belong to the RAD21/REC8 family of chromosome cohesin proteins. Gene 271:99–108

Eijpe M, Offenberg H, Jessberger R et al (2003) Meiotic cohesin REC8 marks the axial elements of rat synaptonemal complexes before cohesins SMC1β and SMC3. J Cell Biol 160: 657–670

Garcia-Cruz R, Brieno MA, Roig I, et al (2010) Dynamics of cohesin proteins REC8, STAG3, SMC1β and SMC3 are consistent with a role in sister chromatid cohesion during meiosis in human oocytes. Human Reproduction: deq180.

Gerhard DS, Wagner L, Feingold EA et al (2004) The status, quality, and expansion of the NIH full-length cDNA project. Genome Res 14:2121–2127

Goldstein P (1987) Multiple synaptonemal complexes (polycomplexes): origin, structure and function. Cell Biol Int Rep 11:759–796

Golubovskaya IN, Hamant O, Timofejeva L et al (2006) Alleles of afd1 dissect REC8 functions during meiotic prophase I. J Cell Sci 119:3306–3315

Golubovskaya IN, Wang CJ, Timofejeva L, Cande WZ (2011) Maize meiotic mutants with improper or non-homologous synapsis due to problems in pairing or synaptonemal complex formation. J Exp Bot 62:1533–1544

Gong C, Li T, Li Q, Yan L, Wang T (2011) Rice OsRAD21-2 is expressed in actively dividing tissues and its ectopic expression in yeast results in aberrant cell division and growth. J Integr Plant Biol 53:14–24

Haering CH, Nasmyth K (2003) Building and breaking bridges between sister chromatids. BioEssays 25:1178–1191

Hartsuiker E, Vaessen E, Carr A, Kohli J (2001) Fission yeast Rad50 stimulates sister chromatid recombination and links cohesion with repair. EMBO J 20:6660–6671

Heckmann S, Schroeder-Reiter E, Kumke K, Ma L, Nagaki K, Murata M, Wanner G, Houben A (2011) Holocentric chromosomes of *Luzula elegans* are characterized by a longitudinal centromere groove, chromosome bending, and a terminal nucleolus organizer region. Cytogenet Genome Res 134: 220–228

Heckmann S, Jankowska M, Schubert V, Kumke K, Ma W, Houben A (2014a) Alternative meiotic chromatid segregation in the holocentric plant *Luzula elegans*. Nat Commun 5:4979

Heckmann S, Schubert V, Houben A (2014b) Holocentric plant meiosis: first sisters, then homologues. Cell Cycle 13:3623–3624

Henderson KA, Keeney S (2005) Synaptonemal complex formation: where does it start? BioEssays 27:995–998

Herran Y, Gutierrez-Caballero C, Sanchez-Martin M et al (2011) The cohesin subunit RAD21L functions in meiotic synapsis and exhibits sexual dimorphism in fertility. EMBO J 30: 3091–3105

Ishiguro K, Kim J, Fujiyama-Nakamura S, Kato S, Watanabe Y (2011) A new meiosis-specific cohesin complex implicated in the cohesin code for homologous pairing. EMBO Rep 12: 267–275

Ishii T, Sunamura N, Matsumoto A et al (2015) Preferential recruitment of the maternal centromere-specific histone H3 (CENH3) in oat (*Avena sativa* L.) × pearl millet (*Pennisetum glaucum* L.) hybrid embryos. Chromosom Res 23:709–718

Jiang L, Xia M, Strittmatter LI, Makaroff CA (2007) The *Arabidopsis* cohesin protein SYN3 localizes to the nucleolus and is essential for gametogenesis. Plant J 50:1020–1034

Kaitna S, Pasierbek P, Jantsch M, Loidl J, Glotzer M (2002) The aurora B kinase AIR-2 regulates kinetochores during mitosis and is required for separation of homologous chromosomes during meiosis. Curr Biol 12:798–812

Klein F, Mahr P, Galova M, Buonomo SB, Michaelis C, Nairz K, Nasmyth K (1999) A central role for cohesins in sister chromatid cohesion, formation of axial elements, and recombination during yeast meiosis. Cell 98:91–103

Kudo NR, Wassmann K, Anger M et al (2006) Resolution of chiasmata in oocytes requires separase-mediated proteolysis. Cell 126:135–146

Kudo NR, Anger M, Peters AH et al (2009) Role of cleavage by separase of the Rec8 kleisin subunit of cohesin during mammalian meiosis I. J Cell Sci 122:2686–2698

Lee J, Hirano T (2011) RAD21L, a novel cohesin subunit implicated in linking homologous chromosomes in mammalian meiosis. J Cell Biol 192:263–276

Lee JY, Orr-Weaver TL (2001) The molecular basis of sister-chromatid cohesion. Annu Rev Cell Dev Biol 17:753–777

Lee J, Iwai T, Yokota T et al (2003) Temporally and spatially selective loss of Rec8 protein from meiotic chromosomes during mammalian meiosis. J Cell Sci 116:2781–2790

Llano E, Gómez R, Gutiérrez-Caballero C et al (2008) Shugoshin-2 is essential for the completion of meiosis but not for mitotic cell division in mice. Genes Dev 22:2400–2413

Losada A, Hirano M, Hirano T (2002) Cohesin release is required for sister chromatid resolution, but not for condensin-mediated compaction, at the onset of mitosis. Genes Dev 16:3004–3016

Marques A, Ribeiro T, Neumann P et al (2015) Holocentromeres in *Rhynchospora* are associated with genome-wide centromere-specific repeat arrays interspersed among euchromatin. Proc Natl Acad Sci 112:13633–13638

Michaelis C, Ciosk R, Nasmyth K (1997) Cohesins: chromosomal proteins that prevent premature separation of sister chromatids. Cell 91:35–45

Mito Y, Sugimoto A, Yamamoto M (2003) Distinct developmental function of two *Caenorhabditis elegans* homologs of the cohesin subunit Scc1/Rad21. Mol Biol Cell 14:2399–2409

Moraes IC, Lermontova I, Schubert I (2011) Recognition of *A. thaliana* centromeres by heterologous CENH3 requires high similarity to the endogenous protein. Plant Mol Biol 75:253–261

Nabeshima K, Villeneuve AM, Colaiácovo MP (2005) Crossing over is coupled to late meiotic prophase bivalent differentiation through asymmetric disassembly of the SC. J Cell Biol 168:683–689

Nagaki K, Kashihara K, Murata M (2005) Visualization of diffuse centromeres with centromere-specific histone H3 in the holocentric plant *Luzula nivea*. Plant Cell 17:1886–1893

Nasmyth K (2011) Cohesin: a catenase with separate entry and exit gates? Nat Cell Biol 13:1170–1177

Nasmyth K, Haering CH (2005) The structure and function of SMC and kleisin complexes. Annu Rev Biochem 74: 595–648

Page SL, Hawley RS (2003) Chromosome choreography: the meiotic ballet. Science 301:785–789

Pasierbek P, Jantsch M, Melcher M, Schleiffer A, Schweizer D, Loidl J (2001) A *Caenorhabditis elegans* cohesion protein with functions in meiotic chromosome pairing and disjunction. Genes Dev 15:1349–1360

Qiao H, Lohmiller LD, Anderson LK (2011) Cohesin proteins load sequentially during prophase I in tomato primary microsporocytes. Chromosom Res 19:193–207

Sakuno T, Tada K, Watanabe Y (2009) Kinetochore geometry defined by cohesion within the centromere. Nature 458: 852–858

Sanei M, Pickering R, Kumke K, Nasuda S, Houben A (2011) Loss of centromeric histone H3 (CENH3) from centromeres precedes uniparental chromosome elimination in interspecific barley hybrids. Proc Natl Acad Sci 108:E498–E505

Schägger H, Von Jagow G (1987) Tricine-sodium dodecyl sulfate-polyacrylamide gel electrophoresis for the separation of proteins in the range from 1 to 100 kDa. Anal Biochem 166:368–379

Schubert V (2009) SMC proteins and their multiple functions in higher plants. Cytogenet Genome Res 124:202–214

Schubert I, Dolezel J, Houben A, Scherthan H, Wanner G (1993) Refined examination of plant metaphase chromosome structure at different levels made feasible by new isolation methods. Chromosoma 102:96–101

Schubert V, Weissleder A, Ali H, Fuchs J, Lermontova I, Meister A, Schubert I (2009) Cohesin gene defects may impair sister chromatid alignment and genome stability in *Arabidopsis thaliana*. Chromosoma 118:591–605

Shao T, Tang D, Wang K et al (2011) OsREC8 is essential for chromatid cohesion and metaphase I monopolar orientation in rice meiosis. Plant Physiol 156:1386–1396

Smolikov S, Schild-Prufert K, Colaiácovo MP (2008) CRA-1 uncovers a double-strand break-dependent pathway promoting the assembly of central region proteins on chromosome axes during *C. elegans* meiosis. PLoS Genet 4, e1000088

Spurr AR (1969) A low-viscosity epoxy resin embedding medium for electron microscopy. J Ultrastruct Res 26:31–43

Sumara I, Vorlaufer E, Stukenberg PT et al (2002) The dissociation of cohesin from chromosomes in prophase is regulated by Polo-like kinase. Mol Cell 9:515–525

Suzuki G, Nishiuchi C, Tsuru A, Kako E, Li J, Yamamoto M, Mukai Y (2013) Cellular localization of mitotic RAD21 with repetitive amino acid motifs in *Allium cepa*. Gene 514:75–81

Sym M, Engebrecht J, Roeder GS (1993) ZIP1 is a synaptonemal complex protein required for meiotic chromosome synapsis. Cell 72:365–378

Tao J, Zhang L, Chong K, Wang T (2007) OsRAD21-3, an orthologue of yeast RAD21, is required for pollen development in *Oryza sativa*. Plant J 51:919–930

Valdeolmillos AM, Viera A, Page J et al (2007) Sequential loading of cohesin subunits during the first meiotic prophase of grasshoppers. PLoS Genet 3, e28

Waizenegger IC, Hauf S, Meinke A et al (2000) Two distinct pathways remove mammalian cohesin from chromosome arms in prophase and from centromeres in anaphase. Cell 103:399–410

Wang M, Tang D, Wang K, Shen Y, Qin B, Miao C, Li M, Cheng Z (2011) OsSGO1 maintains synaptonemal complex stabilization in addition to protecting centromeric cohesion during rice meiosis. Plant J 67:583–594

Weisshart K, Fuchs J, Schubert V (2016) Structured illumination microscopy (SIM) and photoactivated localization microscopy (PALM) to analyze the abundance and distribution of RNA polymerase II molecules on flow-sorted *Arabidopsis* nuclei. Bio-protocol 6, e1725

Westergaard M, von Wettstein D (1972) The synaptonemal complex. Annu Rev Genet 60:533–554

Xu H, Beasley M, Verschoor S et al (2004) A new role for the mitotic RAD21/SCC1 cohesin in meiotic chromosome cohesion and segregation in the mouse. EMBO Rep 5:378–384

Zetka MC, Kawasaki I, Strome S, Müller F (1999) Synapsis and chiasma formation in *Caenorhabditis elegans* require HIM-3, a meiotic chromosome core component that functions in chromosome segregation. Genes Dev 13:2258–2270

Zhang LR, Tao JY, Wang T (2004) Molecular characterization of OsRAD21-1, a rice homologue of yeast RAD21 essential for mitotic chromosome cohesion. J Exp Bot 55:1149–1152

Zhang L, Tao J, Wang S, Chong K, Wang T (2006) The rice OsRad21-4, an orthologue of yeast Rec8 protein, is required for efficient meiosis. Plant Mol Biol 60:533–554